LUMINOSITY STABILITY, POSSIBLE FEEDBACK, AND BACKGROUND AT FUTURE LINEAR COLLIDERS

O. Napoly, CEA/Saclay, France

Abstract

This paper describes the current ideas to take up the challenge of establishing collisions, with high luminosity and good background conditions, of beams with nanometer spot sizes at the interaction point of a future linear collider. Examples are presented from the design work at the different collider projects around the world[1].

1 INTRODUCTION

Next to the centre of mass energy $\sqrt{s}$, luminosity is the second figure of merit of high energy colliders: to compensate the $1/s$ decay of the cross-sections of elementary processes, the average luminosity $\mathcal{L}$ must be of the order of $10^{34}\,\mathrm{cm}^{-2}\mathrm{s}^{-1}$. As shown by Table 1 which selects design parameters of the main projects, this has the two major consequences:

1. horizontal/vertical beam sizes at the interaction point (IP) must be in the submicron/nanometer range;
2. beam-beam forces are very strong and initiate the beamstrahlung effect [2] which degrades the beam energy resolution and generate intense backgrounds.

The IP beam sizes set the scale of the alignment precision and stability required to establish collisions. As discussed in Sec.2, it is essential to understand the nature of the magnet motions and to characterize their time and spatial variations. Since bunch trains are mandatory to produce this high luminosity, the different choices for the pulse repetition frequency f_r, bunch distance $\Delta\tau_B$ and pulse length $N_B\Delta\tau_B$, motivated by the different RF acceleration options, will determine the reach and effectiveness of the beam based feedback systems.

Table 1: Some collider design parameters[1]

	TESLA	NLC/JLC	CLIC
$\sqrt{s}$ [TeV]	0.5	1.0	3.0
$\mathcal{L}$ [$10^{34}\,\mathrm{cm}^{-2}\mathrm{s}^{-1}$]	3.2	1.3	10.0
$\overline{\mathcal{L}}$ [mbarn^{-1}]	2300	1100	6500
N [10^{10}]	2	0.95	0.4
σ_x^* [nm],σ_y^* [nm]	553 , 5	235 , 4	43 , 1
σ_z [μm]	400	120	30
f_r [Hz]	5	120	100
N_B	2820	95	154
$\Delta\tau_B$ [ns]	337	2.8	0.67
Υ	0.04	0.3	8.7
$\langle B\rangle$ [T]	360	1300	12000

Ideally the tolerances to magnet errors should be based on the induced relative luminosity loss. The intensity of the beam-beam forces makes such predictions rely on computer simulations[3] which calculate the single bunch luminosity $\overline{\mathcal{L}}$, given for relativistic beams by the overlap of their
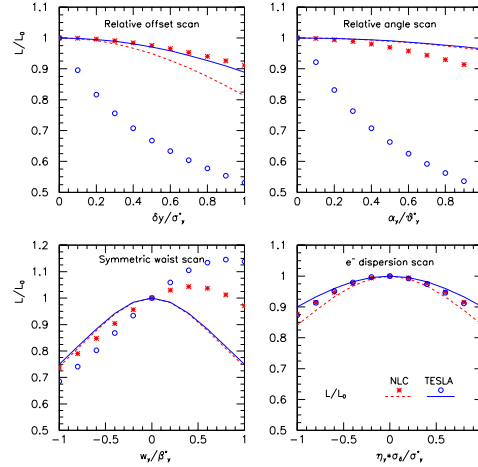

Figure 1: Relative luminosity versus vertical beam offset, angle, waist-shift and dispersion, for the cases of NLC ($\star$,solid) and TESLA ($\circ$,dashed). Simulations[3] are compared to the analytic expectation for rigid Gaussian bunches

current densities $\mathbf{J}_{1,2} = (\rho c, \rho\overrightarrow{v})$:

$$\overline{\mathcal{L}} = 1/c^2 \int d^4\mathbf{x}\,\mathbf{J}_1\cdot\mathbf{J}_2 \simeq 2\int c\,dt\,d^3\overrightarrow{x}\,\rho_1(\overrightarrow{x},t)\,\rho_2(\overrightarrow{x},t)$$

with discretized time steps to include the effect of the beam pinching during the collision. Fig.1 plots the relative luminosity for various beam mismatches at the IP as compared to the analytic calculation for rigid Gaussian beams[4] Even when the sensitivity to small *orbit errors* is greatly enhanced by the beam-beam forces, up to a factor 10 in the case of TESLA due to the large vertical disruption, the *relative* effect of a *beam matrix mismatch* can be predicted by its analytic expression to a sufficient accuracy to specify tolerances. Notice that beam-beam forces increase the luminosity when waists are shifted symmetrically in front of the IP.

Beamstrahlung, i.e. emission of synchrotron radiation in the coherent field of the opposite beam, was observed and used for beam monitoring at the SLC. The intensity of the beam-beam force $2ec\langle B\rangle$ is measured by the Υ parameter[2] given by

$$\Upsilon = \gamma\langle B\rangle/B_S = \frac{5r_e^2\gamma N}{6\alpha(\sigma_x^* + \sigma_y^*)\sigma_z}$$

where $B_S = m_e^2c^2/e\hbar = 4.4\times 10^9$ T. In the very large bending fields expected at the future colliders (cf. Table 1), beamstrahlung photons create e^+e^- pairs and hadrons. In the $\Upsilon > 1$ multi-TeV designs, a large fraction of the photons and pairs carry almost all the electron energy.

Beam-beam and machine backgrounds (cf. Sec.3) can degrade the detector performance. Detector hardware can be damaged by radiation and, at the software level, backgrounds can wrongly trigger data acquisition or confuse pattern recognition when inducing too high occupancies. Interaction region must be properly designed[5] to shield the tracking chambers which are close to the beam axis. Continuing the use of beamstrahlung, the beam-beam background can serve to monitor the collisions and optimize the luminosity.

2 LUMINOSITY STABILISATION AND FEEDBACK SYSTEMS

To maintain the design luminosity, the beam IP orbit and spot size must be controlled to a fraction of the design spot size. Collisions at 120 Hz of $\sigma_y^* = 650$ nm beams at the SLC, and recent magnet vibration or beam jitter measurements show that a stability of the order of 10-100 nm is obtained on accelerator sites. At the FFTB, a 30 Hz beam jitter of 40 nm at the focus point has been measured[6] and attributed to the last triplet support vibrations, and individual quadrupole resonances in the same range have also been recorded. Pushing this stability down to 1 nm or less, is an intense field of research[8].

2.1 Ground Motion

Ground motion studies [9] identified three types of motions in a tunnel: 1) elastic tidal waves with long wavelengths, 2) systematic displacements or diffusive motion with amplitudes and spatial correlations decaying rapidly at high frequencies, 3) vibrations generated by human activities with resonances in the 1-100 Hz range. Elastic waves are harmless since they produce small relative displacements over short distances. Measurements of the pure seismic motion show that some quiet sites offer a rock stability of 1 nm(0.1 nm) integrating motions with frequency higher than 1 Hz(10 Hz). Larger amplitude but lower frequency motions can be corrected by feedback systems if the beam repetition rate is more than 10 times larger. In such sites, the dangerous fast vibrations arise from human activities.

2.2 Spot size tuning and stabilisation

Critical for spot size detuning are the sextupoles of the chromatic correction whose vertical misalignments generate skew quadrupole errors, and the one-before-last doublet whose generated vertical dispersion is blown up by the last doublet. Even in the most demanding designs, like CLIC at 3 TeV[10], their alignment tolerances are however in the 100 nm range. Injection jitter tolerance in the final focus systems is not set by the transfer optics, with an acceptance of several beam sigmas, but by the collimators whose transverse wake fields degrade the beam emittances. In general, it is a fraction of beam sigma accessible, at these high beta points, to submicron resolution BPMs[11]. A feedback system based on the RF-pulse repetition rate and steering the beam through an orbit set by such high resolution BPMs, can therefore stabilise the nominal spot size, until the accumulated displacements of the machine elements require a global realignment.

This assumes that the IP spot size is actually measured, in a time shorter than the lifetime of the correction. Unlike the horizontal one, the vertical spot size cannot be measured by beam-beam deflection scans unless they are compared to a parametrization of extensive multiparameter beam-beam simulations taking the large vertical disruption into account. Beam-beam measurements can be used to directly optimize the convoluted spot size $\Sigma_y = \sqrt{\sigma_y^{(+)2} + \sigma_y^{(-)2}}$ by maximizing the linear part of the vertical beam-beam deflection, or the luminosity $\mathcal{L} \propto 1/\Sigma_y$ by maximizing a beam-beam signal. Probing a luminosity-related signal around its maximum with small deviations of optics tuning parameters is the essence of the luminosity dithering feedback[12] introduced at the SLC which surpasses the beam-beam deflection scan technique in tuning accuracy and luminosity uptime. Beam size and luminosity monitors based on beam-beam signals are discussed in Sect.3.

In the case where the beam-beam tuning fails to obtain the desired luminosity, the separate tuning of each beam lines will be required with a beam size monitor close to the IP. The laser interferometer is presently the only instrument able to measure nanometer spot sizes, although at the very limit of its dynamic range with the present-day laser wavelengths[13].

2.3 IP orbit stabilisation

To stabilise the IP relative beam orbit in the subnanometer range, novel techniques must be developed. One idea is to anchor the sensitive magnets to the stable bedrock[14]: their mechanical vibrations are monitored by laser interferometry and corrected by calibrated piezomovers. In particular, the displacement δy_D and δy_F of the F and D quadrupoles of the last doublet induce the following IP offset

$$\delta y^* = R_{34}(F)g_F\delta y_F + R_{34}(D)\delta y_D$$

where $g_{F,D}$ are the integrated quadrupole strengths. Since the doublet is parallel-to-point focusing, a global doublet offset δy_0 induces an equal IP offset :

$$\delta y^* = (g_F R_{34}(F) + g_D R_{34}(D))\delta y_0 \simeq \delta y_0.$$

For closeby F and D quadrupoles, $g_F R_{34}(F) \simeq 2$ and $g_F R_{34}(F) \simeq -1$, showing that both the F and D quadrupoles must be stabilised. In addition, the two stabilised supports of the facing doublets should be as correlated as possible to function like a common rigid support.

Another idea is to operate fast intra-pulse orbit corrections to cancel the fast motions and beam jitter with frequencies smaller than $1/\tau_B$. The effectiveness of such a feedback system depends on the number of corrections implemented within one bunch train: it is thus very demanding in fast DSP electronics and fast kickers. For TESLA,

the setpoint is a zero difference-orbit between in and out beams, thus canceling the IP beam-beam kick. The pulse to pulse stability is then relaxed up to 200 nm for a 10% luminosity loss[15]. For NLC the setpoint must be predetermined by luminosity measurements and the stability is 10 nm for 4% luminosity loss[16]. Both systems must be supplemented by an IP-angle orthogonal feedback system located in front of the chromaticity correction. Indeed TESLA luminosity is as sensitive to offsets than to angles, when normalized to beam sigmas. For NLC, since the IP angle is not reconstructed to make the correction faster, an IP angle error can confuse the beam-beam angle arising from an offset error.

Beam-beam effects can affect the performance the fast feedback systems. When the vertical disruption is large, the y, y' vs. z bunch correlations caused by linac wakefields move the luminosity optimum to *non-zero* IP relative orbit and angle. If these correlations are stable enough, a fast luminosity monitor can find the optimum and teach the new offsets to the feedback system. Another way would be to directly use the luminosity signal to drive the feedback system in place of the BPMs.

3 BEAM-BEAM BACKGROUNDS AND LUMINOSITY MONITORING

Table 2: Beamstrahlung parameters[17]: average energy loss, number of photons per electron, number of pair particles per bunch crossing and their average energy, their hit density and the neutron flux on the 1st layer of vertex detector, (main beam dump not included for TESLA)

	TESLA	NLC/JLC	CLIC
δ_B [%]	2.8	9.1	31
N_γ/N_e	1.6	1.5	2.3
N_{pairs}/BX	1.6×10^5	9.2×10^4	8×10^8
$\langle E_{\text{pairs}} \rangle$ [GeV]	1.9	10.5	570
N_{hits}/mm^2/BX	0.09 at 4T	0.02 at 6T	0.005 at 4T
N_n [cm^{-2}/year]	3×10^8	2×10^9	—

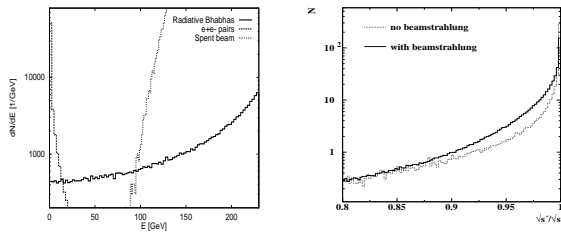## 3.1 Beamstrahlung and spent beam

Figure 2: Spectrum of low energy charged particles (right) and luminosity spectrum $d\mathcal{L}/d\sqrt{s}$ (left) for TESLA at $\sqrt{s} = 500$ GeV

In the beamstrahlung effect, large beam-beam deflection angles combine with large energy losses. The spent beam losses are therefore primarily induced by the overfocussing of the low energy particles in the extraction quadrupoles. As shown in Fig.2, the low energy spectrum of the spent beam joins the spectrum of less energetic e^+e^- pairs and radiative Bhabhas, emitted at even larger angles. The extraction optics must provide enough beam stayclear to limit the energy deposited by these charged particles to an acceptable level. The beamstrahlung photons carry several percent of the total beam power in a very narrow, less than 1 mrad, cone. They can easily be cleared outside of the detector. However dedicated collimation and dump systems are required to handle this power and protect the magnets and instrumentation in the beam extraction line.
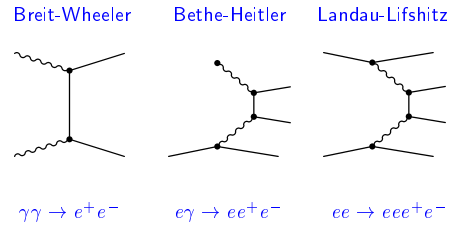
3.2 Electron Positron Pairs

Figure 3: Incoherent processes for e^+e^- pair production

e^+e^- pairs are produced by the three incoherent processes shown in Fig.3. Their rate is therefore proportional to the e^+e^-, $e^\pm\gamma$ and $\gamma\gamma$ luminosities, the last two being built up by the beamstrahlung photons. Depending on their sign, the low energy pair particles are strongly deflected or focussed by the opposite beam. To protect the detector a strong solenoid field must be used to focus most of the pairs down the beam pipe into a forward mask. Fields of 3 T or more are needed to accommodate a vertex detector around the IP with 1 cm radius. Above a few GeV energy, they are transported further down and are stopped or backscattered by the quadrupoles of the extraction line. A high-Z outer mask must absorb the photons produced by showers with about 100 keV energy before they penetrate tracker and calorimeters. An inner mask around the beam axis, with the proper material and aperture, must shield the vertex detector from the backscattered pairs and external machine background. With such masks, the detector background level given in Table 2 are believed to be acceptable. In multi-TeV designs with $\Upsilon > 1$, beamstrahlung photons interacting 'coherently' on the external e.m. field of the opposite beam, generate pairs nearly as many and as energetic as the beam itself[18]. In this regime, beam and pair extraction would require an optics with $\pm$ 100 % momentum bandwidth which in addition must blow up the spot size of the non-interacting, very low emittances beam on the dump.

On the positive side, the high rate of *incoherent* pairs can be used for efficient machine tuning. A beam size monitor has been studied[19] based on measuring the topology of the pair particle hits with a pixel detector around the beam axis. The beam horizontal spot size σ_x and aspect ratio
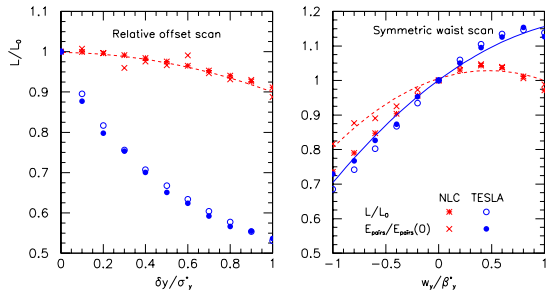
Figure 4: Relative luminosity versus vertical beam offset and waist-shift for the cases of NLC (red,⋆,solid) and TESLA (blue,○,dashed) compared to the signal obtained from the total energy of the pairs.

at the IP can then be inferred by comparison with beam-beam simulations. More directly, the relative luminosity can be monitored with a calorimeter located at 5-25 mrad angles in the mask[20]. Fig.4 shows that the total energy of the pairs follows closely the relative luminosity variations for both orbit or beam size detunings. Parabolic fits like shown in Fig.4 can reconstruct the optimum luminosity with an relative accuracy better than 10^{-3} with only 10 bunch crossings per scan. Such a calorimeter can be read out in 30-50 ns and could therefore be included in a fast correction system fed back directly by luminosity.

3.3 Radiative Bhabhas : $e^+e^- \to e^+e^-\gamma$

With luminosity scaling with s, this process still provides counting rates around 10^3 per bunch crossing, adequate for fast luminosity measurement, even if it is roughly halved[21] by the finite beam size suppression factor. Because of the beam-beam deflection, the rate of low energy electrons into some detector angular acceptance is no longer directly given by the corresponding integral of the differential cross-section $d\sigma/dEd\theta_e$, and it no longer provides an absolute measurement of the luminosity. However, when a usable energy window exists as shown in Fig.2, it can be used as a relative measurement to monitor the luminosity against beam size variations and linear optics tuning[20]. In contrast, the radiated photons are unaffected by the beam-beam forces. Measuring the highest energy part of their spectrum would permit a high precision determination of the absolute luminosity, and also of the IP beam divergence and polarization[21]. Extracting this signal in the forward direction from the intense background of lower energy beamstrahlung photons would be extremely profitable.

3.4 Neutrons

Neutrons are an indirect consequence of the beam-beam effect: they are produced via photo-nuclear reactions from shower photons stemming from particle deposition in the interaction region. This includes mostly the pairs and radiative Bhabhas deposited a few meters away from the IP, and the beamstrahlung and spent beam at their dumps. The flux of neutrons backscattered from these sources must be calculated by GEANT or FLUKA98 simulations[5] showing the influence of neutron absorbers (graphite or paraffin) placed around the beam pipe in the mask or in the dump region. A relatively low-Z beam chamber also helps by letting the photons penetrate deeper in the material. The calculated neutrons flux given in Table 2 are within the safe limit[22] of 3×10^9 cm^{-2} s^{-1} set by the most exposed and fragile CCD based vertex detector.

4 MACHINE BACKGROUNDS

4.1 Beam gas and Thermal photons

In a single pass collider, the main consequences of scattering on residual gas or thermal photons are (i) halo formation in the linac and beam delivery system, and (ii) off-momentum electrons or positrons which confuse the detector low angle tagging ($\theta \sim 25 - 50$ mrad from the IP). At 250 GeV beam energy, the rates of beam-gas bremsstrahlung and Compton scattering on thermal photons cross over[23] at about 10^{-7} Pa of CO gas pressure, for an electron energy loss of 1%, typical of final focus bandwidths. That such a rate has a minor impact on the interaction region and detector has to be confirmed by tracking simulations of beam lines with errors and correctors on.

4.2 Synchrotron radiation

Synchrotron radiation primary hits can be avoided by techniques used at circular colliders : direct collimation of photons radiated from distant dipoles and quadrupoles, collimation of beam tails (both planes, both phases) to clear the photons emitted in the last doublet inside of the detector. In contrast, the use of soft bends to remove the hard photons becomes length costly since, at 500 GeV beam energy, a 3×10^{-4} T field corresponds to 50 keV critical energy, at the limit of the efficiently absorbed soft photon spectrum, and to 5600 km bending radius. Another problem specific to the linear colliders is the magnitude of the synchrotron radiation generated by the disrupted beam in the extraction doublet. For the same beam energy and about 30 μrad beam angular spread, typical values for the incoming doublet synchrotron radiation are : one photon per electron with about 10 MeV critical energy yielding about 100 W average power for Gaussian beams. After beam-beam disruption, the outgoing beam divergences can be 10 times larger : as a consequence ten times more photons with ten times more energy are generated in the outgoing doublet at horizontal angles reaching 1 mrad in the defocussing quadrupole. This is the most powerful source of photon deposition near the detector. It is therefore important to study if the intensity of backshone photons in the inner part of the detector is not too large.

4.3 Muons

Both sign muons, produced by the beam halo hitting small apertures, essentially the collimators, can travel easily to
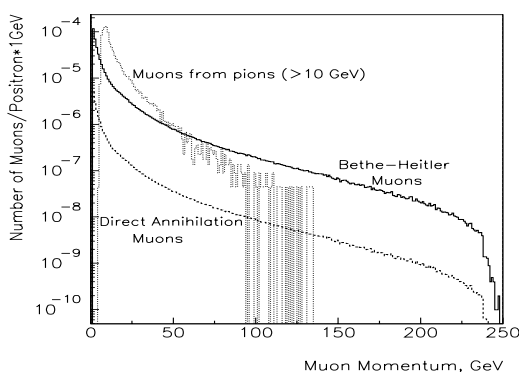
Figure 5: Cross-sections for muon production

the detector. Not to confuse the pattern recognition, a safe limit is a few muons per readout time of the slowest tracking chambers. As shown by Fig.5, high energy muons are mostly produced in pairs by the Bethe-Heitler process (cf. Fig.3). The total rate is quasi-doubled by adding pion production and Bethe-Heitler production from secondaries. At the source, the muon rate is about 2×10^{-5} per lost 250 GeV electron or positron. The muon rate at the detector then scales with the beam halo population and the muon attenuation achieved on the way to the detector. The predicted relative halo population is controversial but low energy collimation should be implemented in front of the linacs to reduce it. Simulations[5] show that tunnel length alone provides about a factor 10 muon attenuation per kilometer. Factors of 100-10000 higher attenuations can be obtained by deflecting the muons with tunnel filling iron toroids like at the SLC, or channeling the both sign muons into iron around the beam pipe with either two nested iron cylinders with opposite toroidal magnetizations, or sequences of small iron toroids with alternate polarities.

5 CONCLUSION

The subnanometer stability required by the future linear colliders is not excluded by natural ground motion, but it will have to be enforced by mechanical stabilisation of magnets and by beam fast feedback systems acting within the bunch trains. At the present stage, both beam-beam and accelerator backgrounds in the $\Upsilon < 1$ designs are acceptable to the detector and IR region. Typical background distributions and events have been already included in detector Monte-Carlo simulations for studying their impact on physics analysis. Luminosity should be the preferred on-line signal not only to improve but also to monitor the operation and the performance of a future linear collider, in contrast with beam size IP measurements. This was already shown in the last year of operation of the SLC. The future linear colliders will profit from even more powerful signals, essentially from the e^+e^- pairs, directly proportional to the luminosity.

6 REFERENCES

[1] Linear Collider Workshop LC99, Frascati, (1999) http://wwwsis.lnf.infn.it/lc99/Proceedings/proceedings.htm

[2] P. Chen and K. Yokoya, "Beam-beam phenomena in linear colliders", KEK-91-002, (1991)
T. Tauchi at al, Part.Accel.**41**, 29 (1993).

[3] P. Chen et al, CAIN, Nucl.Instrum.Meth. A**355**, 107 (1995)
D. Schulte, GUINEA-PIG, PhD Thesis, TESLA-97-08 (1996).

[4] O. Napoly, Part. Accel.**40/4**, 181 (1993).

[5] JLC, NLC and TESLA interaction regions are described in the LCWS99 proceedings, Sitges, Spain (1999).

[6] M. Woods et al., "Vertical position stability of the FFTB electron beam measured by the KEK BSM monitor", FFTB note 98-03 (1998).

[7] P. Raimondi et al., "Recent luminosity improvements at the SLC", EPAC98, Stockholm, Sweden (1998)

[8] R. Assmann et al., "Stability Considerations for final focus systems of future linear colliders", these proceedings.

[9] A. Sery, "Recent ground motion studies at SLAC", these proceedings.
C. Montag, "Ground Motion Measurements in a HERA interaction region", these proceedings.

[10] F. Zimmermann et al., "Final focus system for CLIC at 3 TeV", these proceedings.

[11] T. Slaton et al., "Development of nanometer resolution C-band frequency beam position monitors in the final focus test beam", LINAC98, Chicago, USA, (1998)
V. Balakin et al., "Experimental results from a microwave cavity beam position monitor", PAC99, New York,USA (1999)

[12] P. Emma et al., "Limitations of interaction point spot size tuning at the SLC", PAC97, Vancouver, Canada (1997).
L. Hendrikson et al., "Luminosity optimization feedback at the SLC", SLAC-PUB-8027 (1999).

[13] S. Schreiber, "Instrumentation at the interaction region of a linear e^+e^- collider", LCWS99, Sitges, Spain (1999)

[14] T. Markiewicz et al, "Vibration control of the NLC final doublet", these proceedings.

[15] I. Reyzl, "Stabilisation of beam interaction in the TESLA linear collider", these proceedings.

[16] D. Schulte, "Simulations of Intra-Pulse Interaction Point Feedback for NLC" CLIC Note 415 (1999).

[17] D. Schulte, "Backgrounds at Future Linear Colliders", CERN-PS-99-69 (1999).

[18] D. Schulte, "High energy beam-beam effects in CLIC", PAC99, New-York, USA (1999).

[19] T. Tauchi and K. Yokoya, Phys.Rev.E **51**, 6119 (1995).

[20] O. Napoly and D. Schulte, "Luminosity monitor studies for TESLA", CEA/Saclay preprint DAPNIA-SEA-97-14 (1997).

[21] K. Piotrzkowski, "High energy bremsstrahlung at TESLA", LCWS99, Sitges, Spain (1999).

[22] C. Damerell, private communication

[23] H. Burkhard, "Machine backgrounds common to all Machine", LCWS99, Sitges, Spain (1999).